Journal of Computational Science &Engineering 43 (2019) 1069-1076

Available at http://www.asocse.org ISSN 1710-4068

Direction vector model and block format numerical method for multi-body system dynamics

Zhen Wang[1], Jieyu Ding [1,2*]

[1]School of Mathematics and Statistics, Qingdao University, Qingdao 266071, China

[2]Center for Computational Mechanics and Engineering Simulation, Qingdao University, Qingdao 266071, China

Abstract: The direction vector method is used to describe the dynamic model of multi-body system. The DAEs of index 3 is transformed into the equation of index 2 or 1. The L-stable block format and the Multi-step block format are constructed to simulate the dynamics of the multi-body system for a long time. The simulation results show that the L-stable block format and the Multi-step block format can solve the equations of index 1, 2 and 3 under the same time step size. And the results are better than the classical Runge-kutta method in maintaining the energy error, displacement constraint, velocity constraint and acceleration constraint. The L-stable block scheme constructed by Chebyshev polynomials is better than the L-stable block scheme constructed by equidistant nodes for solving the DAEs with index 3. L-stable block format and Multi-step block format can still maintain good calculation accuracy, which can overcome the disadvantage of Runge-kutta method under the long time simulation.

Keywords: Multi-body system dynamics; Direction vector method; Differential-algebraic equations; L- stable block format; Multi-step block format

Received 9 July 2019, Revised 18 September 2019, Accepted 20 September 2019

*Corresponding Author: Jieyu Ding, djy@qdu.edu.cn

1. Introduction

Mechanism is one of the main categories for optimization design and behavior analysis of engineering systems, which is embodied in complex mechanical systems such as robot, automobile, spacecraft and robot arm. A multibody system is a system of objects connected by motion pairs.The establishment of dynamic model can select different coordinates, such as relative coordinates, absolute coordinates, lie group coordinates and natural coordinates, among which the natural coordinates are also called complete cartesian coordinates. In the 1980s, the natural coordinate method was proposed and developed by Garcia de Jalon[1]. It consists of several basis points and cartesian components of the unit basis vector. It is characterized by flexible selection of coordinates, moderate number of coordinates, linear constraint on Jacobi matrix, and free of costolian inertial force and centrifugal force. The direction vector method belongs to the natural coordinate method, which was proposed and developed by Von Schwerin, Kraus and Uhlar[2-4]. In addition, the direction vector method has good compatibility with absolute coordinates and which is easy to program. The ordinary differential or differential algebraic equations (DAEs) are established according to the principle of dynamics through selecting coordinates, setting system variables, and analyzing the multi-body system. The conventional solution to DAEs is to turn them into ordinary differential equations. The index theory given by Gear, Petzold, and Brennan[5-6] is most often used to analyze the similarity between the two equations.These traditional methods control numerical damping for stability, but reduce the format precision. In terms of accuracy and stability, the research on block format is worth popularizing.

This paper deals with block formats including L-stable block format and Multi-step block format. The L-stable block format is based on the Taylor expansion structure of the exact solution at a certain time. Ehle[7] proposed L-stable based on A-stable and Padé approximation on the basis of ordinary differential solution. The Multi-step block format is a new class of general linear methods with Runge-Kutta stability, constructed based on the general linear method proposed by Butcher[8] and using more past information. Chollom[9] proposed a method to detect the performance of the whole block format and determined the convergence, stability and order of the constructed format. Olabode[10] used the point collocation method to solve the initial value problems of special ordinary differential equations using the block linear Multi-step method in the predictive corrector model. Mehrkanoon[11] proposed a four-point implicit Multi-step block format for solving the first order ordinary differential equation with variable step size and gave a simple form of Adams, which was realized by the gauss-seidel method. Based on the first order ordinary differential solution, Mehrkanoon[12] directly solved the third order ordinary differential equation with variable step size, and studied the local truncation error of the method. Based on the collocation method of approximate solutions of power series and the continuous linear Multi-step block method of interpolation method, Awoyemi[13] improves the existing block format to adapt to the general N order ordinary differential

2019@ The American Computational Science Society. All rights reserved.

equations. Abdul Majid[14] used one-step method to solve second-order ordinary differential equations without reducing the equation to first-order equations. Olabode[15] studied self starting block format method, do not need to develop a single predictor. Mohamed[16] combined the third-order multi-step block method with the newton-cotes method to solve the second type of linear and nonlinear integro-differential equations.

At present, the L-stable block format and the Multi-step block format are more based on ordinary differential equations, and the research on DAEs is less. The DAEs of multi body system dynamics are described by direction vector method. Construct L stable block format and Multi step block format for numerical calculation. The maximum energy error, displacement constraint, velocity constraint and acceleration constraint are analyzed and compared. Based on the zero point of Chebyshev polynomial, the unequal distance node block format is constructed, and the simulation experiment is carried out through the slider-crank mechanism.

2. DAEs of Multibody system dynamics by the direction vector method

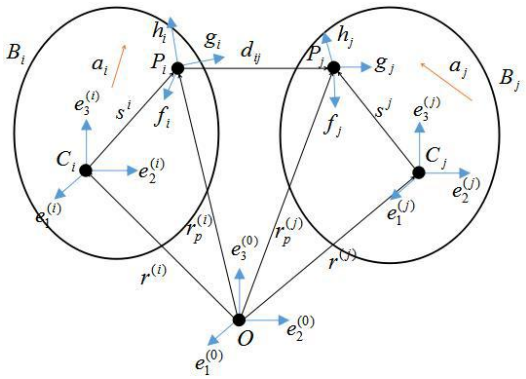

Fig.1 Schematic diagram of any two multibody systems and hinges

Assuming that system is made up of n_i objects and n_j hinges connection of the multibody system. In Fig.1, Establish coordinate $\boldsymbol{C}_i\boldsymbol{e}_1^{(i)}\boldsymbol{e}_2^{(i)}\boldsymbol{e}_3^{(i)}$ at the center of mass C_i of object $B_i(i=1,2\cdots n)$. The origin of C_i relative position vector C_i is $\boldsymbol{O}\boldsymbol{e}_1^{(0)}\boldsymbol{e}_2^{(0)}\boldsymbol{e}_3^{(0)}$ .The kinetic energy of the $B_i(i=1,2\cdots n)$ is

$$T_i=\frac{1}{2}\int_V \rho\dot{\boldsymbol{r}}_p^{(i)\mathrm{T}}\dot{\boldsymbol{r}}_p^{(i)}dV=\frac{1}{2}\dot{\boldsymbol{r}}^{(i)\mathrm{T}}m_i\boldsymbol{E}\dot{\boldsymbol{r}}^{(i)} +\frac{1}{2}\sum_{j=1}^{3}\dot{\boldsymbol{e}}_j^{(i)\mathrm{T}}\Pi_j\dot{\boldsymbol{e}}_j^{(i)}=\frac{1}{2}\dot{\boldsymbol{q}}^{(i)}\boldsymbol{M}_i\dot{\boldsymbol{q}}^{(i)} \tag{1}$$

Where $\dot{\boldsymbol{r}}_p^{(i)}=\dot{\boldsymbol{r}}^{(i)}+\sum_{j=1}^{3}x_j\dot{\boldsymbol{e}}_j^{(i)}$ is speed of any point P on B_i, $\boldsymbol{q}^{(i)}=[\boldsymbol{r}^{(i)\mathrm{T}},\boldsymbol{e}^{(i)\mathrm{T}}]^{\mathrm{T}}$, $\boldsymbol{r}^{(i)}=[r_1^{(i)},r_2^{(i)},r_3^{(i)}]^{\mathrm{T}}$, $\boldsymbol{e}^{(i)}=[\boldsymbol{e}_1^{(i)\mathrm{T}},\boldsymbol{e}_2^{(i)\mathrm{T}},\boldsymbol{e}_3^{(i)\mathrm{T}}]^{\mathrm{T}}$, $\boldsymbol{e}_j^i=[\boldsymbol{e}_{1j}^{(i)\mathrm{T}},\boldsymbol{e}_{2j}^{(i)\mathrm{T}},\boldsymbol{e}_{3j}^{(i)\mathrm{T}}]^{\mathrm{T}}$, and $\boldsymbol{M}_i=diag(m_i\boldsymbol{E},\Pi_1^{(i)}\boldsymbol{E},\Pi_2^{(i)}\boldsymbol{E},\Pi_3^{(i)}\boldsymbol{E})$, $m_i=\int_V\rho dV$, $\Pi_j^{(i)}=\int_V\rho x_j^2dV$. The potential energy of $B_i(i=1,2\cdots n)$ is $V_i=\boldsymbol{V}(\boldsymbol{q}^{(i)})$.

The constraint is divided into two parts: the constraint of direction vector property and the constraint of hinge between objects. The constraint of direction vector property is

$$\boldsymbol{\Phi}^{(i)}=\begin{bmatrix}\frac{1}{2}(\boldsymbol{e}_1^{(i)T}\boldsymbol{e}_1^{(i)}-1)\\ \frac{1}{2}(\boldsymbol{e}_2^{(i)T}\boldsymbol{e}_2^{(i)}-1)\\ \frac{1}{2}(\boldsymbol{e}_3^{(i)T}\boldsymbol{e}_3^{(i)}-1)\\ \boldsymbol{e}_1^{(i)T}\boldsymbol{e}_2^{(i)}\\ \boldsymbol{e}_1^{(i)T}\boldsymbol{e}_3^{(i)}\\ \boldsymbol{e}_2^{(i)T}\boldsymbol{e}_3^{(i)}\end{bmatrix} \tag{2}$$

As shown in Figure 1,the constraint of hinge between objects is

a. $\boldsymbol{a}_i,\boldsymbol{a}_j$ is any vector,when they're vertical to each other, $\boldsymbol{\Phi}(\boldsymbol{a}_i,\boldsymbol{a}_j)=\boldsymbol{a}_i^{\mathrm{T}}\boldsymbol{a}_j=0$;

b. $\boldsymbol{d}_{ij}$ is the relative position vector between two points , when they're vertical to each other , $\boldsymbol{\Phi}(\boldsymbol{a}_i,\boldsymbol{d}_{ij})=\boldsymbol{a}_i^{\mathrm{T}}\boldsymbol{d}_{ij}=0$;

c. P_i,P_j is the hinge points of B_i,B_j ,when coincide, $\boldsymbol{\Phi}(P_i,P_j)=\boldsymbol{r}_p^{(j)}-\boldsymbol{r}_p^{(i)}=0$;

d. When the distance between P_i and P_j remains the same , $\boldsymbol{\Phi}(P_i,P_j)=\boldsymbol{d}_{ij}^{\mathrm{T}}\boldsymbol{d}_{ij}-C^2=0$;

e. $p_if_ig_ih_i,p_jf_jg_jh_j$ coordinates on the points P_i,P_j ,When $\boldsymbol{h}_i,\boldsymbol{h}_j$ are parallel vectors, $\boldsymbol{\Phi}(\boldsymbol{h}_i,\boldsymbol{h}_j)=\begin{bmatrix}\boldsymbol{\Phi}(\boldsymbol{f}_i,\boldsymbol{h}_j)\\ \boldsymbol{\Phi}(\boldsymbol{g}_i,\boldsymbol{h}_j)\end{bmatrix}=0$;

f. when $\boldsymbol{h}_i,\boldsymbol{d}_{ij}$ are parallel vectors, $\boldsymbol{\Phi}(\boldsymbol{h}_i,\boldsymbol{d}_{ij})=\begin{bmatrix}\boldsymbol{\Phi}(\boldsymbol{f}_i,\boldsymbol{d}_{ij})\\ \boldsymbol{\Phi}(\boldsymbol{g}_i,\boldsymbol{d}_{ij})\end{bmatrix}=0$;

Similar ball hinge, universal hinge, rotating hinge, barrel hinge and sliding hinge can be expressed by the

2019@ The American Computational Science Society. All rights reserved.

above six inter-hinge constraints.

The principle of Lagrange-d'Alembert:

$$\delta\sum_{i=1}^{n_i}\int_0^T(\frac{1}{2}\dot{\boldsymbol{q}}^{(i)\mathrm{T}}\boldsymbol{M}_i\dot{\boldsymbol{q}}^{(i)}-\boldsymbol{V}(\boldsymbol{q}^{(i)})-\boldsymbol{\lambda}^{(i)\mathrm{T}}\boldsymbol{\Phi}^{(i)})dt-$$
$$\delta\sum_{l=1}^{n_l}\int_0^T\delta\boldsymbol{\lambda}_l^{\mathrm{T}}\boldsymbol{\Phi}_l dt+\sum_{i=1}^{n_l}\int_0^T\delta\boldsymbol{q}^{(i)\mathrm{T}}\boldsymbol{F}(\boldsymbol{q}^{(i)})dt=0 \tag{3}$$

Using a matrix describe：

$$\delta\int_0^T(\frac{1}{2}\dot{\boldsymbol{q}}^{\mathrm{T}}\boldsymbol{M}\dot{\boldsymbol{q}}-\boldsymbol{V}(\boldsymbol{q})-\boldsymbol{\lambda}^{\mathrm{T}}\boldsymbol{\Phi}(\boldsymbol{q}))dt$$
$$+\int_0^T\delta\boldsymbol{q}^{\mathrm{T}}\boldsymbol{F}(\boldsymbol{q})dt=0 \tag{4}$$

Where $\boldsymbol{q}=[\boldsymbol{q}^{(1)\mathrm{T}},\boldsymbol{q}^{(2)\mathrm{T}},\cdots,\boldsymbol{q}^{(n_i)\mathrm{T}}]^{\mathrm{T}}$,

$\boldsymbol{M}=diag(\boldsymbol{M}_1,\boldsymbol{M}_2,\cdots,\boldsymbol{M}_{n_i})$, $\boldsymbol{V}(\boldsymbol{q})=\sum_{i=1}^{n_i}\boldsymbol{V}(\boldsymbol{q}^{(i)})$,

$\boldsymbol{F}(\boldsymbol{q})=[\boldsymbol{F}(\boldsymbol{q}^{(1)})^{\mathrm{T}},\boldsymbol{F}(\boldsymbol{q}^{(2)})^{\mathrm{T}},\cdots,\boldsymbol{F}(\boldsymbol{q}^{(n_i)})^{\mathrm{T}}]^{\mathrm{T}}$,

$\boldsymbol{\lambda}$ is Lagrange multiplier, $\boldsymbol{\Phi}(\boldsymbol{q})$ is constraint function.

The DAEs of index-3 in multibody systems dynamics are

$$\begin{cases}\boldsymbol{M}\ddot{\boldsymbol{q}}+\boldsymbol{\Phi}_q^{\mathrm{T}}\boldsymbol{\lambda}=\boldsymbol{F}(\boldsymbol{q})-\dfrac{\partial\boldsymbol{V}}{\partial\boldsymbol{q}}\\ \boldsymbol{\Phi}(\boldsymbol{q})=0\end{cases} \tag{5}$$

For the constraint equation $\boldsymbol{\Phi}$,the first derivative and the second derivative are respectively obtained for the time t,and the DAEs form of the index-2 and the index-1 can be obtained by the combination of (5).

$$\begin{cases}\boldsymbol{M}\ddot{\boldsymbol{q}}+\boldsymbol{\Phi}_q^{T}\boldsymbol{\lambda}=\boldsymbol{F}(\boldsymbol{q})-\dfrac{\partial\boldsymbol{V}}{\partial\boldsymbol{q}}\\ \boldsymbol{\Phi}_q(\boldsymbol{q})\dot{\boldsymbol{q}}+\boldsymbol{\Phi}_t(\boldsymbol{q})=0\end{cases} \tag{6}$$

$$\begin{cases}\boldsymbol{M}\ddot{\boldsymbol{q}}+\boldsymbol{\Phi}_q^{\mathrm{T}}\boldsymbol{\lambda}=\boldsymbol{F}(\boldsymbol{q})-\dfrac{\partial V}{\partial\boldsymbol{q}}\\ \boldsymbol{\Phi}_q(\boldsymbol{q})\ddot{\boldsymbol{q}}+[\boldsymbol{\Phi}_{qq}(\boldsymbol{q})\dot{\boldsymbol{q}}]\dot{\boldsymbol{q}}+2\boldsymbol{\Phi}_{qt}(\boldsymbol{q})\dot{\boldsymbol{q}}+\boldsymbol{\Phi}_{tt}(\boldsymbol{q})=0\end{cases} \tag{7}$$

Taking the multibody system dynamics DAEs of index-1 equations (7) as an example after the order reduction the following first-order differential equations can be obtained.

$$\begin{cases}\boldsymbol{z}=\dot{\boldsymbol{q}}\\ \boldsymbol{M}\dot{\boldsymbol{z}}+\boldsymbol{\Phi}_q^{\mathrm{T}}\boldsymbol{\lambda}=\boldsymbol{F}(\boldsymbol{q})-\dfrac{\partial\boldsymbol{V}}{\partial\boldsymbol{q}}\\ \boldsymbol{\Phi}_q(\boldsymbol{q})\dot{\boldsymbol{z}}+[\boldsymbol{\Phi}_{qq}(\boldsymbol{q})\boldsymbol{z}]\boldsymbol{z}+2\boldsymbol{\Phi}_{qt}(\boldsymbol{q})\boldsymbol{z}+\boldsymbol{\Phi}_{tt}(\boldsymbol{q})=0\end{cases} \tag{8}$$

3. Construction of the DAEs L-Stable Format and Multi-body Format

L-stable block format and multi-step block format have similar block format construction ideas: Based on the exact solution of Taylor exhibition type to struct the formula of block format . A single-step interval $[t_i,t_{i+1}]$, slecting $t_i<c_1<c_2<\cdots<c_r=t_{i+1}$, where r is the number of node. Let $\boldsymbol{Y}_i=[\boldsymbol{y}_1^{\mathrm{T}},\boldsymbol{y}_2^{\mathrm{T}},\cdots,\boldsymbol{y}_r^{\mathrm{T}}]$ as the input vector .From the Taylor expansion of $\boldsymbol{y}_k$ in t_i to

$$[\boldsymbol{B},\boldsymbol{d}]=[\boldsymbol{G}][\boldsymbol{P}]^{-1} \tag{9}$$

$$[\boldsymbol{A},\boldsymbol{U}]=\boldsymbol{C}\begin{bmatrix}\boldsymbol{H}\\ \boldsymbol{D}\end{bmatrix}^{-1} \tag{10}$$

Where (9) （10） are the construction matrices of L-stable block format and multi-step block format respectively, and $\boldsymbol{G}=[\boldsymbol{h},\boldsymbol{h}^2,\cdots,\boldsymbol{h}^r,\ \boldsymbol{\mu}]$,

$\boldsymbol{P}=[1,2\boldsymbol{h},3\boldsymbol{h},\cdots,(r-1)\boldsymbol{h}^r]$,

$\boldsymbol{h}=(h_1,h_2,\cdots,h_r)^{\mathrm{T}}$, $\boldsymbol{\mu}=(\mu_1,\mu_2,\cdots,\mu_{\mathrm{r}})^{\mathrm{T}}$;

$\boldsymbol{C}=[\boldsymbol{c},\dfrac{\boldsymbol{c}^2}{2!},\cdots,\dfrac{\boldsymbol{c}^{(2r-1)}}{(2r-1)!}]$,

$\boldsymbol{H}=[0,\dfrac{\boldsymbol{c}}{1!},\cdots,\dfrac{\boldsymbol{c}^{(2r-2)}}{(2r-2)!}]$,

$\boldsymbol{D}=[\boldsymbol{c}-1,\dfrac{(\boldsymbol{c}-1)^2}{2!},\cdots,\dfrac{(\boldsymbol{c}-1)^{(2r-1)}}{(2r-1)!}]$,

$\boldsymbol{c}=(\boldsymbol{c}_1,\boldsymbol{c}_2,\cdots,\boldsymbol{c}_r)^{\mathrm{T}}$, solving equation (9), $\boldsymbol{B}$ and $\boldsymbol{d}$ can be determined in the L-stable block format, and solving equation (10), $\boldsymbol{A}$ and $\boldsymbol{U}$ can be determined in the multi-step block format so that the output value of each moment in the time step can be obtained.

A time step $h=t_{i+1}-t_i$, $c_k(k=1,2,\cdots,r)$ can be an equidistant node or a nonequidistant node, selecting $t_i<c_1<c_2<\cdots<c_r=t_{i+1}$. $\boldsymbol{Y}_i$ is the initial value, make

$$\boldsymbol{Y}_{i+1}=\boldsymbol{e}\otimes\boldsymbol{y}_i+h\boldsymbol{d}\otimes\dot{\boldsymbol{y}}_i+h\boldsymbol{B}\otimes\dot{\boldsymbol{Y}}_{i+1} \tag{11}$$

$$\boldsymbol{Y}_{i+1}=h(\boldsymbol{A}\otimes\boldsymbol{I}_m)\dot{\boldsymbol{Y}}_{i+1}+(\boldsymbol{U}\otimes\boldsymbol{I}_m)\boldsymbol{Y}_i \tag{12}$$

where (11) and (12) are the solution formulas of L-stable block format and multi-step block format respectively, $\boldsymbol{e}=[1,1,\cdots 1]_{1\times r}^{\mathrm{T}}$, $\boldsymbol{I}_m$ is $m\times m$ Unit matrix, $\otimes$ is Kronecker . $\dot{\boldsymbol{Y}}_{i+1}=[\dot{\boldsymbol{y}}_1,\dot{\boldsymbol{y}}_2,\cdots,\dot{\boldsymbol{y}}_r](\dot{\boldsymbol{y}}_k=[\dot{\boldsymbol{q}}_k^{\mathrm{T}},\ddot{\boldsymbol{q}}_k^{\mathrm{T}},\boldsymbol{\lambda}_k])$ obtained by iterative solution of (5) (6) (7), $\boldsymbol{Y}_{i+1}=[\boldsymbol{y}_1^{\mathrm{T}},\boldsymbol{y}_2^{\mathrm{T}},\cdots,\boldsymbol{y}_r^{\mathrm{T}}]^{\mathrm{T}}(\boldsymbol{y}_k=[\boldsymbol{q}_k^{\mathrm{T}},\dot{\boldsymbol{q}}_k^{\mathrm{T}},\bar{\boldsymbol{\lambda}}_k])$ O btained by (11)or(12).

2019@ The American Computational Science Society. All rights reserved.

When $r=3$, $\boldsymbol{c}=(\frac{1}{3},\frac{2}{3},1)^{\mathrm{T}}$, $\boldsymbol{\mu}=(\frac{1}{45},\frac{8}{45},1)^{\mathrm{T}}$, in the (11) formula,

$$\boldsymbol{B}=\frac{1}{3}\begin{bmatrix}\frac{107}{120} & -\frac{37}{120} & \frac{3}{40}\\ \frac{17}{15} & \frac{8}{15} & -\frac{1}{15}\\ \frac{9}{8} & \frac{9}{8} & \frac{3}{8}\end{bmatrix},\boldsymbol{d}=\frac{1}{3}\begin{bmatrix}\frac{41}{120}\\ \frac{2}{5}\\ \frac{3}{8}\end{bmatrix};$$

in the (12) formula,

$$\boldsymbol{A}=\frac{1}{5832}\begin{bmatrix}4381 & -2654 & 691\\ 5302 & -1508 & 586\\ 5029 & -62 & 1339\end{bmatrix},$$

$$\boldsymbol{U}=\frac{1}{648}\begin{bmatrix}-137 & 432 & 353\\ -134 & 432 & 350\\ -137 & 432 & 353\end{bmatrix}.$$

According to the tectonic process, select the zero of the Chebyshev polynomial, so

$$\boldsymbol{c}=(\frac{1}{2}-\frac{\sqrt{2}}{4},\frac{1}{2}+\frac{\sqrt{2}}{4},1)^{\mathrm{T}},$$

$$\boldsymbol{\mu}=(\frac{10-5\sqrt{2}}{32},\frac{10+5\sqrt{2}}{32},\frac{1}{2}+\frac{\sqrt{2}}{4})^{\mathrm{T}},$$

$$\boldsymbol{B}=\begin{bmatrix}\frac{11-2\sqrt{2}}{24} & \frac{5-8\sqrt{2}}{24} & \frac{7\sqrt{2}-1}{48}\\ \frac{5+8\sqrt{2}}{24} & \frac{11+2\sqrt{2}}{24} & -\frac{7\sqrt{2}+1}{48}\\ \frac{2}{3} & \frac{2}{3} & -\frac{1}{6}\end{bmatrix},$$

$$\boldsymbol{d}=\begin{bmatrix}\frac{\sqrt{2}-7}{48}\\ -\frac{\sqrt{2}+7}{48}\\ -\frac{1}{6}\end{bmatrix};$$

Select different nodes, substitute the $\boldsymbol{B}$ and $\boldsymbol{d}$ obtained by the construction method into equation (11), $\boldsymbol{A}$ and $\boldsymbol{U}$ into equation (12), determine L-stable block format and multi-step block format, and obtain the initial value of the next time period.

4. Numerical example

Crank-slider mechanism is shown in Figure 1;the length of the link is L_1, L_2,where $L_1=0.5\mathrm{m}$, $L_2=1\mathrm{m}$, and the quality is m_1, m_2, m_3,where $m_1=10kg$, $m_2=20kg$, $m_3=20kg$. For the convenience of calculation, the conjoined basis coordinates along the principal axis of inertia are established at the center of mass of each object.

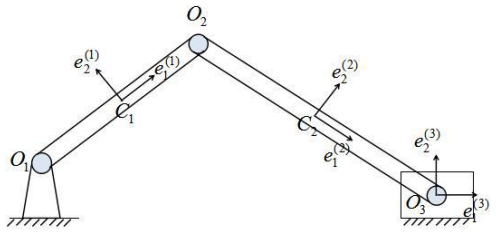

Fig.2 Slider-crank mechanism

For any bar, Generalized coordinates is $\boldsymbol{q}^{(i)}=[\boldsymbol{r}^{(i)\mathrm{T}},\boldsymbol{e}^{(i)\mathrm{T}}]^{\mathrm{T}}$, $\boldsymbol{r}^{(i)}=[r_1^{(i)},r_2^{(i)}]^{\mathrm{T}}$, $\boldsymbol{e}^{(i)}=[e_1^{(i)\mathrm{T}},e_2^{(i)\mathrm{T}}]^{\mathrm{T}}$, $r_2^3=0$, Generalized mass matrix is

$$\boldsymbol{M}_i=\begin{bmatrix}m_i\boldsymbol{E}_2 & & \\ & \Pi_1^{(i)}\boldsymbol{E}_2 & \\ & & \Pi_2^{(i)}\boldsymbol{E}_2\end{bmatrix}_{6\times6} \quad (13)$$

Where m_i is the weight of the bar i,

$$\Pi_1^{(i)}=\int_{-\mathrm{a}/2}^{\mathrm{a}/2}(\int_{-l/2}^{l/2}\rho x_1^2dx_1)dx_2=\frac{m_i}{12}L_i^2,$$

$$\Pi_2^{(i)}=\int_{-l/2}^{l/2}(\int_{-\mathrm{a}/2}^{\mathrm{a}/2}\rho x_2^2dx_2)dx_1=\frac{m_i}{12}\mathrm{a}^2.$$

The system potential energy is

$$\boldsymbol{V}(\boldsymbol{q})=r_2^{(1)}m_1g+r_2^{(2)}m_2g \quad (14)$$

The constraint condition of the direction vector is

$$\boldsymbol{\Phi}^{(i)}=\begin{bmatrix}\frac{1}{2}(\boldsymbol{e}_1^{(i)\mathrm{T}}\boldsymbol{e}_1^{(i)}-1)\\ \frac{1}{2}(\boldsymbol{e}_2^{(i)\mathrm{T}}\boldsymbol{e}_2^{(i)}-1)\\ \boldsymbol{e}_1^{(i)\mathrm{T}}\boldsymbol{e}_2^{(i)}\end{bmatrix} \quad (15)$$

The constraint condition at turning hinge O_1,O_2,O_3 is

$$\begin{cases}\boldsymbol{r}^{(1)}-\frac{L_1}{2}\boldsymbol{e}_1^{(1)}=0\\ \boldsymbol{r}^{(2)}-\frac{L_2}{2}\boldsymbol{e}_1^{(2)}-\boldsymbol{r}^{(1)}-\frac{L_1}{2}\boldsymbol{e}_1^{(1)}=0\\ \boldsymbol{r}^{(2)}+\frac{L_2}{2}\boldsymbol{e}_1^{(2)}-\boldsymbol{r}^{(3)}=0\end{cases} \quad (16)$$

Assumed initial value $\boldsymbol{q}_0=(0.25,0,1,0,0,1,1,0,1,0,0,1,1.5,0)^{\mathrm{T}}$,

2019@ The American Computational Science Society. All rights reserved.

$\dot{q}_0 = (0,\cdots,0)^{\mathrm{T}}_{1\times 12}$ .When the simulation time is 10s, the $r_1^{(i)}, r_2^{(i)}, r_3^{(i)}$ simulation curve is obtained Figure 3.

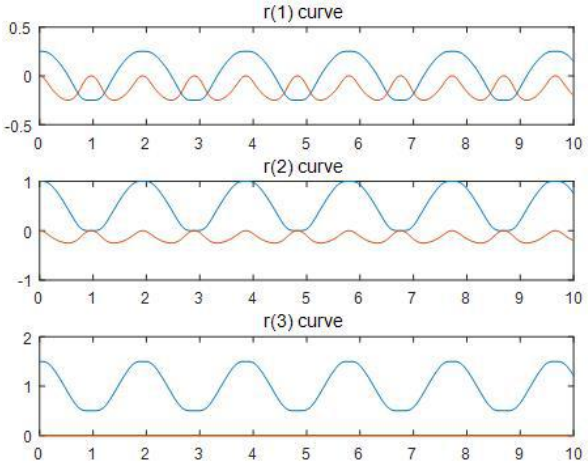

Fig.1 Slider-crank mechanism each vector component simulation curve

（1）When the simulation time is 10s, the L-stable block format and the Multi-step block format are used to solve the index 3 DAEs constructed by equidistant nodes. According to table 1-2, when h is smaller and running time is longer, the maximum energy error is smaller and smaller. The displacement constraint, velocity constraint and acceleration constraint remain stable. Therefore, when the simulation time is fixed, shortening the h can achieve better simulation effect.

（2）Runge-kutta method is only effective for solving index 1 DAEs. So it is particularly important to introduce L-stable block format and Multi-step block format. It can be seen from table 3-4 that the Multi-step block format has no index limit on solving the DAEs. And it maintains a relatively stable state for maximum energy error, displacement constraint, Speed-level constraint and acceleration constraint.

（3）The Runge-kutta method is not effective in maintaining the total energy for a long time. Table 5-10 can be seen that L-stable block format and Multi-step block format can realize long-term simulation for index 1, 2 and 3 equations. The maximum energy error is stable with time and keeping good constraint conditions.

（4）For the solution of index 1 DAEs, Table 11 can be seen that L-stable block format and Multi-step block format overcome the disadvantages of Runge-kutta method in energy retention and long time simulation.

Table 1. Compared with different phase of L-stable block format's results (index 3 DAEs simulation time 10s)

step	runtime	$\|H\|_{\max}$	Constraint function $\boldsymbol{\Phi}$	Speed-level constraint $\boldsymbol{\Phi}_t$	Acceleration-level constrains $\boldsymbol{\Phi}_{tt}$
h=0.01	48.7188	0.0090	4.4409e-16	3.6692e-05	0.0514
h=0.005	88.2656	0.0022	4.4409e-16	4.5512e-06	0.0127
h=0.001	451.2188	8.9780e-05	4.4409e-16	3.6181e-08	5.0653e-04

Table 2. Compared with different phase of Multi-step block format's results (index 3 DAEs simulation time 10s)

step	runtime	$\|H\|_{\max}$	Constraint function $\boldsymbol{\Phi}$	Speed-level constraint $\boldsymbol{\Phi}_t$	Acceleration-level constrains $\boldsymbol{\Phi}_{tt}$
h=0.01	49.4063	0.0028	4.4409e-16	4.5350e-06	0.0046
h=0.005	92.0625	7.1181e-04	4.4409e-16	2.8288e-07	5.7563e-04
h=0.001	485.0313	2.8473e-05	4.4409e-16	5.4344e-10	7.2746e-06

2019@ The American Computational Science Society. All rights reserved.

Table 2. Compared the results of L- stable block format of index 1, 2 and 3 (simulation time 10s phase 0.01)

	runtime	$\|H\|_{max}$	Constraint function $\boldsymbol{\Phi}$	Speed-level constraint $\boldsymbol{\Phi}_t$	Acceleration-level constrains $\boldsymbol{\Phi}_{tt}$
index-1	54.0156	0.0039	1.5946e-05	1.7594e-06	1.0658e-14
index-2	51.2500	0.0019	9.0328e-09	1.3323e-15	9.7471e-04
index-3	45.9063	0.0019	4.4409e-16	4.8381e-05	0.0248

Table 4. Compared the results of Multi-step block format of index 1, 2 and 3 (simulation time 10s phase 0.01)

	runtime	$\|H\|_{max}$	Constraint function $\boldsymbol{\Phi}$	Speed-level constraint $\boldsymbol{\Phi}_t$	Acceleration-level constrains $\boldsymbol{\Phi}_{tt}$
index-1	54.8125	0.0208	1.4921e-04	1.6919e-05	1.2517e-14
index-2	51.5156	0.0028	1.3492e-07	1.3323e-15	0.0022
index-3	49.4063	0.0028	4.4409e-16	4.5350e-06	0.0046

Table 5. Compared of results of L-stable block format in different simulation time (index 3 DAEs phase 0.01)

Simulation time	runtime	$\|H\|_{max}$	Constraint function $\boldsymbol{\Phi}$	Speed-level constraint $\boldsymbol{\Phi}_t$	Acceleration-level constrains $\boldsymbol{\Phi}_{tt}$
10	45.9063	0.0019	4.4409e-16	4.8381e-05	0.0248
50	229.3594	0.0163	4.4409e-16	4.8454e-05	0.0249
100	449.7813	0.0346	4.4409e-16	4.8474e-05	0.0249

Table 6. Compared of results of Multi-step block format in different simulation time (index 3 DAEs phase 0.01)

Simulation time	runtime	$\|H\|_{max}$	Constraint function $\boldsymbol{\Phi}$	Speed-level constraint $\boldsymbol{\Phi}_t$	Acceleration-level constrains $\boldsymbol{\Phi}_{tt}$
10	49.4063	0.0028	4.4409e-16	4.5350e-06	0.0046
50	242.1406	0.0028	4.4409e-16	4.5351e-06	0.0046
100	482.8281	0.0028	4.4409e-16	4.5351e-06	0.0046

Table 7. Compared of results of L-stable block format in different simulation time (index 2 DAEs phase 0.01)

Simulation time	runtime	$\|H\|_{max}$	Constraint function $\boldsymbol{\Phi}$	Speed-level constraint $\boldsymbol{\Phi}_t$	Acceleration-level constrains $\boldsymbol{\Phi}_{tt}$
10	51.2500	0.0019	9.0328e-09	1.3323e-15	9.7471e-04
50	248.7344	0.0019	3.0310e-08	1.7764e-15	9.7471e-04
100	496.8125	0.0019	5.7296e-08	1.7764e-15	9.7472e-04

2019@ The American Computational Science Society. All rights reserved.

Table 8 Compared of results of Multi-step block format in different simulation time (index 2 DAEs phase 0.01)

Simulation time	runtime	$\|H\|_{\max}$	Constraint function $\boldsymbol{\Phi}$	Speed-level constraint $\boldsymbol{\Phi}_t$	Acceleration-level constrains $\boldsymbol{\Phi}_{tt}$
10	52.2344	0.0028	1.3492e-07	1.3323e-15	0.0022
50	260.0938	0.0028	1.4718e-07	1.7764e-15	0.0022
100	505.5781	0.0028	2.7373e-07	1.7764e-15	0.0022

Table 9. Compared of results of L-stable block format in different simulation time (index 1 DAEs phase 0.01)

Simulation time	runtime	$\|H\|_{\max}$	Constraint function $\boldsymbol{\Phi}$	Speed-level constraint $\boldsymbol{\Phi}_t$	Acceleration-level constrains $\boldsymbol{\Phi}_{tt}$
10	54.0156	0.0039	1.5946e-05	1.7594e-06	1.0658e-14
50	253.5156	0.0118	7.9768e-05	1.7594e-06	1.4502e-14
100	499.8906	0.0216	1.5937e-04	1.7594e-06	1.5488e-14

Table 10. Compared of results of Multi-step block format in different simulation time (index 1 DAEs phase 0.01)

Simulation time	runtime	$\|H\|_{\max}$	Constraint function $\boldsymbol{\Phi}$	Speed-level constraint $\boldsymbol{\Phi}_t$	Acceleration-level constrains $\boldsymbol{\Phi}_{tt}$
10	54.5000	0.0208	1.4921e-04	1.6919e-05	1.2517e-14
50	267.1719	0.0942	7.4552e-04	1.6919e-05	1.4211e-14
100	505.1719	0.1858	0.0015	1.6919e-05	1.5342e-14

Table 11 Compared runge-kutta method with Multi-step block format and L-stable block format（simulation time 100s phase 0.01）

	runtime	$\|H\|_{\max}$	Constraint function $\boldsymbol{\Phi}$	Speed-level constraint $\boldsymbol{\Phi}_t$	Acceleration-level constrains $\boldsymbol{\Phi}_{tt}$
L-stable	499.8906	0.0216	1.5937e-04	1.7594e-06	1.5488e-14
Multi-step block	505.1719	0.1858	0.0015	1.6919e-05	1.5342e-14
Runge-Kutta	13.2656	3.1639	0.0251	5.2151e-04	1.0836e-13

5. Conclusion

Compared with other coordinates modeling methods, the direction vector method has the advantages of flexible selection,simple form easy to understand, more stylized and easy to program. Through the comprehensive comparison of numerical experiments, it can be obtained that the L-stable block

2019@ The American Computational Science Society. All rights reserved.

format constructed by equidistant nodes and the multi-step block format can maintain good results in terms of maximum energy error, displacement constraint, velocity constraint and acceleration constraint of corresponding indexes. And the results obtained are better than the results of runge-kutta method. In addition, the L-stable block format is better for solving the DAEs of index 3 constructed by the zero point of Chebyshev polynomial. In the case of fixed phase, L-stable block format and Multi-step block format are more suitable for long time simulation. Runge-kutta method, a classical algorithm for calculating DAEs, is used to solve the problem. In the case of shorter time simulation and larger phase, the accuracy will be reduced. And the total energy will increase with time. Therefore, in the case of long time simulation, L-stable block format or Multi-step block format can be selected to simulate the DAEs described by the direction vector method.

Acknowledgments

The financial support was provided by the National Natural Science Foundation of China(NNSFC) through grant Nos 11772166,11472143.

References

[1] J.García de Jalón, E. Bayo. Berlin: Springer,1994.
[2] R.V.Schwerin. Berlin:Springer,1999.
[3] C.Kraus, H.G.Bock, H. Mutschler. Multibody System Dynamics, 13(2005): 101-111.
[4] S.Uhlar, P.Betsch. Multibody system dynamics, 22(2009): 69-95.
[5] C.W. Gear, L.R. Petzold. SIAM Journal on Numerical analysis, 21(1984): 716-728.
[6] K.E. Brenan, S.L. Campbell, L.R. Petzold. Siam, 1996.
[7] B.L. Ehle. SIAM Journal on Mathematical Analysis, 4(1973): 671-680.
[8] J.C. Butcher. Mathematics of Computation, 20(1966): 1-10.
[9] J.P. Chollom, J.N. Ndam, G.M. Kumleng. Science world journal, 2(2007):11-17.
[10] B.T. Olabode. Pacific journal of science and technology, 10(2009): 136-142.
[11] S. Mehrkanoon, Z.A. Majid, M. Suleiman. Journal of Computational and Applied Mathematics, 233(2010): 2387-2394.
[12] S. Mehrkanoon. Numerical Algorithms, 57(2011): 53-66.
[13] D.O.A woyemi, E.A. Adebile, A.O. Adesanya. International Journal of Applied Mathematics and Computation, 3(2011): 181-188.
[14] Z.Abdul Majid, N.Z.Mokhtar, M.Suleiman. Mathematical Problems in Engineering, 2012.
[15] B.T. Olabode. FUTA Journal of Research in Sciences, 2(2013): 194-200.
[16] N.A. Mohamed, Z.A. Majid. Malaysian Journal of Mathematical Sciences, 10(2016): 33-48.

2019@ The American Computational Science Society. All rights reserved.